European Conference on Optical Communication (ECOC) 2022 © Optica Publishing Group 2022

Generation of Strong Parametric Fluorescence in a Highly-Nonlinear Silicon Nitride Waveguide With a Simple Pulsed Pump Source

Ping Zhao*, Zhichao Ye, Magnus Karlsson, Victor Torres-Company and Peter A. Andrekson

Photonics Laboratory, Department of Microtechnology and Nanoscience,
Chalmers University of Technology, SE-412 96 Gothenburg, Sweden.
*pingz@chalmers.se

Abstract *We present the generation of strong parametric fluorescence based on the spontaneous four-wave mixing in a highly-nonlinear silicon nitride waveguide pumped by a simple C-band pulsed pump. Parametric fluorescence spanning over 100 nm with a maximum power spectral density of -25 dBm/nm is experimentally achieved. ©2022 The Author(s)*

Introduction

Since it was observed in 1967 [1], optical parametric fluorescence (PF) has been widely employed in many areas including optical coherence tomography [2]–[4], spectroscopy [5], metrology [6], and quantum signal processing [7], [8]. Generally, PF is generated by optically pumping a $\chi^{(2)}$ or $\chi^{(3)}$ nonlinear medium. $\chi^{(2)}$ platforms, such as lithium niobate, are advantageous due to their high nonlinearity which facilitates the use of modest-pump powers [8]. However, these $\chi^{(2)}$-based PF generators rely on cascaded second-order nonlinear optical processes due to their complexity requiring periodic poling to operate [9]. On the other hand, four-wave mixing (FWM) in a $\chi^{(3)}$ nonlinear medium can be directly applied to the generation of PF, in which two pump photons are transferred into a pair of signal and idler photons. For instance, PF can be generated in a highly-nonlinear fiber (HNLF) [10]. Nevertheless, due to the small nonlinearity of HNLF which is also limited by Brillouin scattering [11], hundreds-of meters-long HNLFs were required. In recent years, compact PF generators based on integrated silicon nitride waveguides ($\chi^{(3)}$ platform) are attracting intensive interest [5]. Compared with HNLFs, silicon nitride waveguides exhibit distinct advantages of small footprint, high nonlinearity and excellent flexibility in dispersion engineering. To generate sufficient PF, a femtosecond laser with a peak power over 1400 W was utilized to pump a silicon nitride waveguide as a result of the short waveguide length, i.e., 7 mm [5]. The power spectral density (PSD) was still limited to about -40 dBm/nm. To reduce the requirement on the pump for PF generation, long highly-nonlinear silicon nitride waveguides with low propagation losses are needed, which holds great prospects for optical communication and signal processing [12], [13].

In this report, we experimentally demonstrate PF with a PSD over -25 dBm/nm, using a 1.7-meter-long low-loss highly-nonlinear silicon nitride waveguide and a simple cost-effective pulsed pump source. The pump source is based on the transient response of Erbium-doped fiber amplifiers (EDFAs), with a peak power of only 11 W and a repetition rate of 50 kHz. Moreover, the effective PF bandwidth for SPD higher than -50 dBm/nm reaches more than 100 nm and can be greatly increased in principle via fine engineering of waveguide dispersion [14].

Experimental Setup

The experimental setup of the PF generation is shown in Fig. 1. A continuous-wave (CW) 1545.5 nm pump laser was followed by an acoustic optical modulator (AOM) which was controlled by a 50 kHz periodic rectangular electrical signal

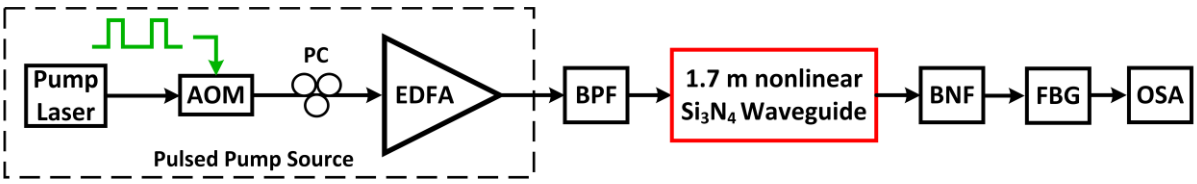

Fig. 1. Diagram of experimental setup of generating PF in a long highly-nonlinear silicon nitride waveguide. Green curve is for temporal waveform of the electrical signal to control an AOM.

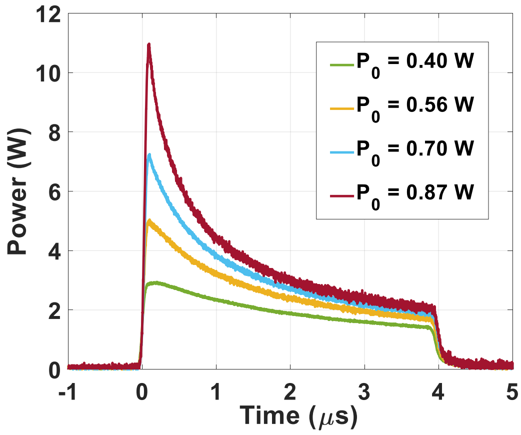

Fig. 2. Temporal waveforms of the pump pulse under various average powers (P_0). The green, orange, blue and red lines are for P_0 = 0.4 W, 0.56 W, 0.70 W, and 0.87 W, respectively.

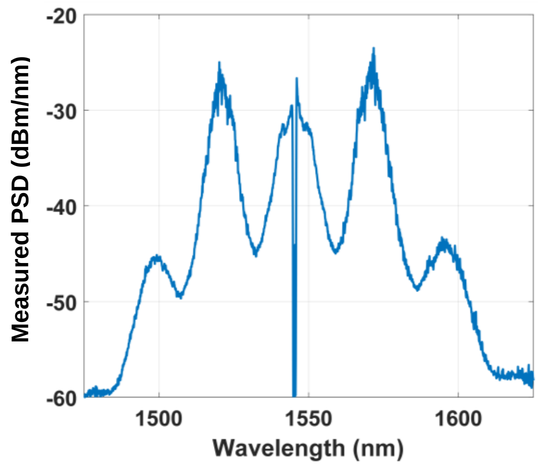

Fig. 3. Measured Optical spectrum of generated PF based on a 1.7-meter-long highly-nonlinear Si_3N_4 waveguide.

with a duty cycle of 20%. The rectangular optical pulses after the AOM were then fed to an EDFA operated in constant-output-power mode. The polarization controller (PC) was used to adjust the polarization state of the pump into the Si_3N_4 waveguide. Before entering the Si_3N_4 waveguide via a lensed fiber, the pulsed pump was processed by a band-pass filter (BPF) with a bandwidth of 1.6 nm to remove most of the amplified spontaneous emission (ASE) generated in the EDFA. In this case, the PF at the output of the Si_3N_4 waveguide can be ultimately undisturbed by the ASE of the EDFA. Besides, we recorded the PF spectrum using an optical spectrum analyser (OSA). To prevent the OSA from being burnt, a band notch filter (BNF) with a bandwidth of 1.6 nm and a fiber Bragg grating (FBG) were utilized to mitigate the residual pump laser component in optical signals at Si_3N_4 the waveguide output. The polarization state of the pump was optimized by maximizing the PSD of the PF.

The highly-nonlinear Si_3N_4 waveguide was 1.7 m long and fabricated following the method in [12]. To generate strong PF, parametric amplification based on FWM is needed. The group velocity dispersion of the fundamental transverse electric (TE_{00}) mode in the Si_3N_4 waveguide was designed to be about -20 ps^2/km at 1550 nm and facilitated the parametric amplification process. Spot-size converters were utilized at both input and output of the waveguide to maximize the coupling efficiency between TE_{00} mode in the Si_3N_4 waveguide and lensed fibers. The coupling loss was about 2 dB/facet. Additionally, the propagation loss of the Si_3N_4 waveguide was about 2.8 dB/m in the C band.

Due to slow response time in the EDFA, an overshoot can be expected, if the duration of an optical pulse is on microsecond scale [15]. Here, this transient effect of EDFA paves the way to increasing the peak power of optical pulses, that is, we can obtain high peak power at the rising edge of the pump pulse for increasing the power of generated PF. In this experiment, each seed pump pulse duration was 4 µs. Fig. 2 depicts the temporal waveforms of the pump pulses with different average power (P_0) after the BPF. In the case of 0.56 W average pump power, a peak pump power of 5 W can be achieved according to the green line plotted in Fig. 2. The pump power decreases monotonically after reaching the peak in the duration time. Additionally, the orange, blue and red lines correspond to an average power of 0.40 W, 0.56 W, 0.70 W, and 0.87 W, respectively. As can be seen, the peak power can reach about 11 W when the average pump power reaches to 0.87 W which is utilized for PF generation. In this way, we obtain a simple cost-effective pulsed pump source with sufficient peak power. With the uncertainty of the coupling loss, we estimate that the peak power in the Si_3N_4 waveguide is 6.2 ~7.8 W.

Experimental Result and Analysis

Fig. 3 presents the measured spectrum of the obtained PF. The resolution of the OSA is 0.1 nm. As it is shown in Fig. 3, the highest PF SPD reaches -23.5 dBm/nm at 1572 nm wavelength which corresponds to one of the phase-matched wavelengths with respect to the pump power. The SPD of the obtained PF at the other phase-matched wavelength of 1520 nm is -25 dBm/nm. The power difference between the PF signals at two phase-matched wavelengths is attributed to the wavelength-dependent coupling loss which is higher in the blue side of the pump wavelength than that in the red side. Besides, there are two small peaks beyond the phase-matched wavelengths, which is due to the gain side lobes

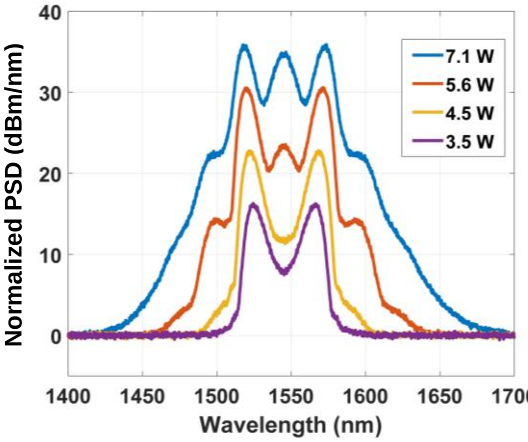

Fig. 4. Relative simulated PSD of PF generated in the Si_3N_4 waveguide with various CW pumps. The purple, orange, red and blue lines correspond to pump powers of 3.5 W, 4.5 W, 5.6 W and 7.1 W, respectively.

of FWM-based parametric amplification [12], [16]. The bandwidth of PF in a PSD higher than -50 dB/nm is 110 nm (1493 nm to 1603 nm). The spectral dip at the 1545 nm wavelength is due to the filters blocking the pump.

To get a better understanding to the PF generation in the Si_3N_4 waveguide, we performed numerical simulations based on the nonlinear Schrödinger equation [11]. Raman and Brillouin scattering effects are neglected. We only consider the second-order dispersion and set the effective nonlinear coefficient (γ) of TE_{00} mode to be 1 $(Wm)^{-1}$. The pump power at the waveguide input is constant in the simulation, instead of being pulsed. The noise source we consider here is vacuum fluctuation with random phases as initial condition [17]. Fig. 4 presents the simulated PF spectra for different pump powers (P_0). The PF spectra are normalized by the minimum PSD. We perform 100 individual simulations and average the spectra to obtain the envelop of the spectrum of simulated PF for a given pump power. The purple, orange, red and blue lines correspond to a pump power of 3.5 W, 4.5 W, 5.6 W and 7.1 W, respectively. The pump components on the simulated spectra are neglected. As can be seen in Fig. 4, the spectrum of PF exhibits a typical feature of parametric amplification for a pump power of 3.5 W. With the increase in the pump power, the peak PSD rises, and the wavelength difference ($\Delta\lambda$) in the spectral peak of the PF and the pump wave is enlarged according to phase-matching condition, $\Delta\lambda \propto \gamma P_0$. For a pump power of 5.6 W, the simulated spectrum agrees with the experimental spectrum. Slight discrepancies in the spectral shape between the simulation and experiment are attributed to the actual dispersion and loss variations along the meter-scale waveguide due to fabrication tolerances and weak multimode interference [12]. Moreover, there is a spectral peak near the pump wavelength. Further increasing the pump power leads to more enhancement of the PSD near the pump wavelength than at the phase-matching wavelength. This indicates that high pump power can help to reduce the spectrum fluctuation of the PF generated in nonlinear Si_3N_4 waveguides.

Conclusions

Strong PF was experimentally realized by pumping a 1.7-meter-long dispersion-engineered highly-nonlinear Si_3N_4 waveguide using a simple cost-efficient pulsed optical source. We obtained a maximum SPD of -23.5 dBm/nm and an effective bandwidth of 110 nm. The experimental result is in accordance with the theoretical expectation. Improved dispersion engineering can in principle further expand the bandwidth of the Si_3N_4-waveguide-based PF generation which can find applications in various areas such as optical tomography, metrology and quantum optics.

Acknowledgements

We wish to thank Mr. Yan Gao for his help on processing the chips and the financial support from the Swedish Research Council (grant VR-2015-00535, VR-2020-00453).

References

[1] S. E. Harris, M. K. Oshman, and R. L. Byer, "Observation of Tunable Optical Parametric Fluorescence," *Physical Review Letters*, vol. 18, no. 18, pp. 732–734, 1967, DOI: 10.1103/PhysRevLett.18.732.

[2] J. Le Gouët, D. Venkatraman, F. N. C. Wong, and J. H. Shapiro, "Classical low-coherence interferometry based on broadband parametric fluorescence and amplification," *Optics Express*, vol. 17, no. 20, pp. 17874–17887, 2009, DOI: 10.1364/OE.17.017874.

[3] G. J. Machado, G. Frascella, J. P. Torres, and M. V Chekhova, "Optical coherence tomography with a nonlinear interferometer in the high parametric gain regime," *Applied Physics Letters*, vol. 117, no. 9, p. 94002, 2020, DOI: 10.1063/5.0016259.

[4] A. Vanselow, P. Kaufmann, I. Zorin, B. Heise, H. M. Chrzanowski, and S. Ramelow, "Frequency-domain optical coherence tomography with undetected mid-infrared photons," *Optica*, vol. 7, no. 12, pp. 1729–1736, 2020, DOI: 10.1364/OPTICA.400128.

[5] N. M. Lüpken, T. Würthwein, J. P. Epping, K.-J. Boller, and C. Fallnich, "Spontaneous four-wave mixing in silicon nitride waveguides for broadband coherent anti-Stokes Raman scattering spectroscopy," *Optics Letters*, vol. 45, no. 14, pp. 3873–3876, 2020, DOI: 10.1364/OL.396394.

[6] A. Riazi, E. Y. Zhu, C. Chen, A. V. Gladyshev, P. G.

Kazansky, and L. Qian, “Alignment-free dispersion measurement with interfering biphotons,” *Optics Letters*, vol. 44, no. 6, pp. 1484–1487, 2019, DOI: 10.1364/Ol.44.001484.

[7] C. Kurtsiefer, M. Oberparleiter, and H. Weinfurter, “High-efficiency entangled photon pair collection in type-II parametric fluorescence,” *Physical Review A - Atomic, Molecular, and Optical Physics*, vol. 64, no. 2, p. 4, 2001, DOI: 10.1103/PhysRevA.64.023802.

[8] N. Takanashi, A. Inoue, T. Kashiwazaki, T. Kazama, K. Enbutsu, R. Kasahara, T. Umeki, and A. Furusawa, “All-optical phase-sensitive detection for ultra-fast quantum computation,” *Optics Express*, vol. 28, no. 23, pp. 34916–34926, 2020, DOI: 10.1364/Oe.405832.

[9] S.-K. Shen, A.-Y. Yang, L. Zuo, J.-M. Cui, and Y.-N. Sun, “Temperature-dependent second harmonic generation process based on an MgO-doped periodically poled lithium niobate waveguide,” *Chinese Physics B*, vol. 20, no. 10, p. 104206, 2011, DOI: 10.1088/1674-1056/20/10/104206.

[10] R. Tang, J. Lasri, P. S. Devgan, V. Grigoryan, P. Kumar, and M. Vasilyev, “Gain characteristics of a frequency nondegenerate phase-sensitive fiber-optic parametric amplifier with phase self-stabilized input,” *Optics Express*, vol. 13, no. 26, pp. 10483–10493, 2005, DOI: 10.1364/OPEX.13.010483.

[11] G. Agrawal, *Nonlinear Fiber Optics*, Fifth Ed. Academic, 2013. DOI: 10.1016/B978-0-12-397023-7.00005-X.

[12] Z. Ye, P. Zhao, K. Twayana, M. Karlsson, Torres-Company Victor, and Andrekson Peter A., “Overcoming the quantum limit of optical amplification in monolithic waveguides,” *Science Advances*, vol. 7, no. 38, p. eabi8150, 2021, DOI: 10.1126/Sciadv.Abi8150.

[13] P. Zhao, M. Karlsson, and P. A. Andrekson, “Low-Noise Integrated Phase-Sensitive Waveguide Parametric Amplifiers,” *Journal of Lightwave Technology*, vol. 40, no. 1, pp. 128–135, 2022, DOI: 10.1109/JLT.2021.3119423.

[14] P. Zhao, Z. Ye, K. Vijayan, C. Naveau, J. Schröder, M. Karlsson, and P. A. Andrekson, “Waveguide tapering for improved parametric amplification in integrated nonlinear Si3N4 waveguides,” *Optics Express*, vol. 28, no. 16, pp. 23467–23477, 2020, DOI: 10.1364/OE.389159.

[15] A. K. Srivastava, Y. Sun, J. L. Zyskind, and J. W. Sulhoff, “EDFA transient response to channel loss in WDM transmission system,” *IEEE Photonics Technology Letters*, vol. 9, no. 3, pp. 386–388, 1997, DOI: 10.1109/68.556082.

[16] M. Pu, H. Hu, L. Ottaviano, E. Semenova, D. Vukovic, L. K. Oxenløwe, and K. Yvind, “Ultra-Efficient and Broadband Nonlinear AlGaAs-on-Insulator Chip for Low-Power Optical Signal Processing,” *Laser and Photonics Reviews*, vol. 12, no. 12, p. 1800111, 2018, DOI: 10.1002/Lpor.201800111.

[17] R. Paschotta, “Noise of mode-locked lasers (Part I): numerical model,” *Applied Physics B*, vol. 79, no. 2, pp. 153–162, 2004, DOI: 10.1007/S00340-004-1547-X.